Letter

Critical slowing down in sudden quench dynamics

Ceren B. Dağ,[1,2,*,†] Yidan Wang,[2,*] Philipp Uhrich,[3] Xuesen Na,[4] and Jad C. Halimeh[3]
[1]*ITAMP, Harvard-Smithsonian Center for Astrophysics, Cambridge, Massachusetts 02138, USA*
[2]*Department of Physics, Harvard University, 17 Oxford Street Cambridge, Massachusetts 02138, USA*
[3]*Pitaevskii BEC Center, CNR-INO and Dipartimento di Fisica, Università di Trento, I-38123 Trento, Italy*
[4]*Department of Mathematics, University of Illinois Urbana-Champaign, 1409 W Green St, Urbana, Illinois 61801, USA*

(Received 14 October 2021; revised 13 October 2022; accepted 2 February 2023; published 28 March 2023)

We reveal a prethermal dynamical regime upon suddenly quenching to the vicinity of a quantum phase transition in the time evolution of one-dimensional spin chains. The prethermal regime is analytically found to be self-similar and its duration is governed by the ground-state energy gap. Based on analytical insights and numerical evidence, we show that this dynamical regime universally exists independently of the location of the probe site, the presence of weak interactions, or the initial state. The resulting prethermal dynamics leads to an out-of-equilibrium scaling function of the order parameter in the vicinity of the transition. Our theory suggests that sudden quench dynamics, besides probing quantum phase transitions, may give rise to a *universal critical slowing down* near the critical point.

DOI: 10.1103/PhysRevB.107.L121113

Introduction. Out-of-equilibrium quantum many-body physics has recently been at the forefront of theoretical and experimental investigations in condensed matter physics [1] due to recent impressive progress in the control and precision achieved in quantum synthetic matter [2–11]. Not only have concepts from equilibrium physics been extended to the out-of-equilibrium realm such as with dynamical phase transitions [12–16] and dynamical scaling laws [14,17–22], but there have also been concerted efforts to probe equilibrium quantum critical points (QCPs) and universal scaling laws through quench dynamics [17,19,21,23–29] or with infinite-temperature initial states [30–32]. Such techniques obviate the need for undertaking the usually difficult task of cooling the system into its ground state over a range of its microscopic parameters to construct its equilibrium phase diagram. The underlying concept behind these works is of the Landau paradigm [12], i.e., it is based on nonanalytic behavior in the long-time dynamics of a local order parameter. This indicates that, in principle, such nonanalytic behavior may be used to extract equilibrium criticality that manifests itself dynamically.

It is well known that relaxation times of order parameters diverge at QCP after slow quenches [9,33,34]. Such divergent behavior of the order parameter is a signature of the nonanalyticity at the QCP and is often referred to as *critical slowing down*. While the current focus of the literature is to utilize sudden quenches in probing the QCP, how the relaxation time of the order parameter behaves around the QCP after a sudden quench has not been sufficiently explored [19,21,33,35–37]. In fact, intriguingly, it has been found that some one-dimensional (1D) short-range models relax the fastest at the QCP [21,33,35,36], contrary to the common intuition of critical slowing down. Dynamical order parameters for these models also do not exhibit nonanalyticity at the QCP [21,36,38].

In this Letter, we introduce boundaries to short-range 1D spin systems and probe single-site order parameters. This reveals a universal prethermal regime upon suddenly quenching to the vicinity of a QCP, when a nonanalyticity of the dynamical order parameter is present at the QCP. Phrased differently, we show the presence of critical slowing down of order parameter dynamics near a QCP after a sudden quench. Intuitively, we find that the duration of the prethermal regime is determined by the inverse energy gap. The universality of the regime holds true for different probe sites, initial conditions, and weak integrability breaking. Further, we analytically and numerically show that this *critically prethermal* regime gives rise to a nonlinear scaling function for the dynamical order parameter in the reduced control parameter of the QCP. We present our discussion based on a paradigmatic model of QCPs, the transverse-field Ising chain (TFIC).

Our work provides new insights on probing quantum criticality in sudden quench dynamics: Quantum criticality does not only affect the stationary regime, but its signature is also visible in a new dynamical regime emerging before the stationary regime. Therefore, sudden quench dynamics does not only probe quantum phase transitions as has been found so far by many [23–27,29,40], but also gives rise to a universal and critical slowing down near QCP.

Dynamical regimes of TFIC. The short-range TFIC with interaction strength Δ is given by

$$H = -J\sum_{r=1}^{N-1}\sigma_r^z\sigma_{r+1}^z - \Delta\sum_{r=1}^{N-2}\sigma_r^z\sigma_{r+2}^z + h\sum_{r=1}^{N}\sigma_r^x, \qquad (1)$$

*These authors contributed equally to this work.
†ceren.dag@cfa.harvard.edu

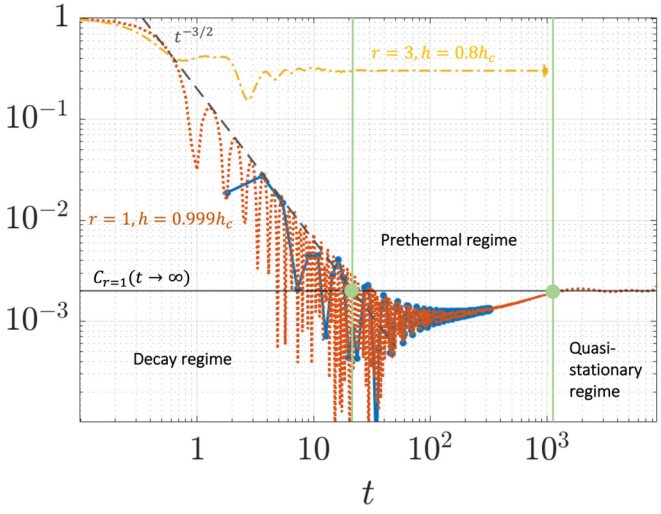

FIG. 1. The edge magnetization $|C_1(t)|$ for the Hamiltonian Eq. (1) with $\Delta = 0$ after a quench in the transverse-field strength from $h_i = 0$ to the vicinity of the QCP at h_c. The red-dotted curve is plotted based on Eq. (3) for a semi-infinite chain [39]. The blue-squares are values of $|C_1(t, h)|$ obtained numerically for the open-boundary TFIC with a system size of $N = 1440$, the method of which is detailed in Ref. [40]. The panels show the three regimes of time evolution separated by green vertical lines: the decay regime with a power-law decay $\sim t^{-3/2}$ (dashed-gray line) on the left, the prethermal regime in the middle and the quasistationary (q.s.) regime on the right. The horizontal black line is $1 - h^2$, the q.s. value for $r = 1$. The onsets of prethermal and q.s. regimes are marked with green balls. As a comparison, the yellow dotted-dashed line plots $|C_{r=3}(t, h)|$ away from the QCP at $h = 0.8h_c$ for $N = 1500$ spins and a quench from $h_i = 0$ where there is no prethermal regime.

where $\sigma_r^{x,z}$ are the Pauli spin matrices on sites r, h is the transverse-field strength, N is the length of the chain, and we fix $J = 1$, which sets the energy scale of the system. In equilibrium, the TFIC has two phases, (i) the ferromagnetically ordered phase for $h < h_c$ and (ii) the paramagnetic disordered phase for $h \geqslant h_c$, where h_c is the QCP. At $\Delta = 0$, this model becomes the nearest-neighbor (n.n.) TFIC with a QCP $h_c = 1$ and the model is integrable. The QCP shifts to favor order upon introducing interactions with $\Delta > 0$. The order parameter for this QCP is the magnetization averaged over all sites; when it is finite, it indicates spontaneous symmetry breaking in the ground state and the system is in the ordered phase.

We consider as an initial state the ground state $|\psi_0\rangle$ of H at initial value h_i of the transverse-field strength and then we quench the latter to a value h. In a periodic chain, the single-site magnetization $C_r(t) = \langle\psi_0|\sigma_r^z(t)|\psi_0\rangle$, at any site r, decays exponentially to zero for any h [21,38,41,42], and hence $C_r(t \to \infty)$ does not host nonanalyticity at the QCP [21,38]. On the other hand, in an open-boundary chain, $C_r(t)$ stabilizes to a finite nonzero value when $t \to \infty$ at any r within a finite distance to the boundary, so long as $h_i < h < h_c$. This dynamical regime is called the quasistationary (q.s.) regime [40,43]; see Fig. 1. For $h \geqslant h_c$, $C_r(t \to \infty) = 0$ is suggested by numerical results [40,43] and some analytical arguments [40]. In our joint paper [40], a kink observed at the QCP becomes sharper as the system size increases and this suggests a nonanalyticity in $C_r(t \to \infty)$. The origin of this nonanalyticity depends on the presence of zero modes which are induced in the open-boundary chain [40]. In particular, for the edge magnetization ($r = 1$) with $\Delta = 0$ and $h_i = 0$, there exists a simple analytic form in the infinite time limit $C_1(t \to \infty) = 1 - h^2 \equiv C_1^{qs}$ for $h < 1$ and $C_1(t \to \infty) = 0$ for $h \geqslant 1$ [40,43,44].

The single-site magnetization at any r away from the QCP approaches the q.s. regime as $t^{-3/2}$ after an exponential decay so long as $h_i < h$ [43]. Upon quenching to the vicinity of the QCP the decay trend is described only by the power law $t^{-3/2}$. Additionally, an intermediate dynamical regime emerges preceding the q.s. regime (see Fig. 1)—the magnetization dips below the q.s. value and eventually ramps up to it. Figure 1 shows the time evolution of the edge magnetization $|C_1(t)|$ when the system is quenched from $h_i = 0$, e.g., $|\psi_0\rangle = |\uparrow\uparrow \ldots \uparrow\rangle$ to $h = 0.999$, in the integrable (n.n.) TFIC both numerically and analytically [39], where we observe this intermediate regime marked as the *prethermal regime*. The onsets t_{pt} and t_{qs} of the prethermal and q.s. regimes, respectively, are where the decay roughly ends, i.e., $t_{pt}^{-3/2} \sim C_1^{qs}$, and where a stationary value is attained in the time evolution, respectively (vertical lines in Fig. 1). To probe and characterize this prethermal regime, we first define a reduced control parameter $h_n \equiv (h_c - h)/h_c$ as the distance to the QCP and $\delta C_r(t, h_n) \equiv C_r[t, h = h_c(1 - h_n)] - C_r(t, h = h_c)$, which we name the *critical response*. As $h_n \to 0$, $C_1^{qs}(h_n) \approx 2h_n$, we arrive at $t_{pt} \propto h_n^{-2/3}$. The central result of our Letter is that when $h_n \to 0$ and $t \gg 1$, the critical response for general r takes the universal form

$$\delta C_r(t, h_n) = C_r^{qs}(|h_n|) f_{\Delta,h_i}(h_n t), \tag{2}$$

where $f_{\Delta,h_i}(h_n t)$ depends on the weak interaction strength Δ [45] and the initial condition h_i. Note that $C_r^{qs}(|h_n|)$ is the q.s. value in the ordered phase, while Eq. (2) works on both sides of the QCP. Furthermore, $f_{\Delta,h_i}(h_n t)$ is a continuous function of $h_n t$ that satisfies $f_{\Delta,h_i}(h_n t = 0) = 1/2$ and $f_{\Delta,h_i}(h_n t) = 1 - f_{\Delta,h_i}(-h_n t)$. When $|h_n|t \gg 1$, $f_{\Delta,h_i}(h_n t)$ approaches 1 in the ordered phase ($h_n > 0$) and approaches 0 in the disordered phase ($h_n < 0$), demonstrating the nonanalyticity in the q.s. value across the QCP. We plot $f_{\Delta,h_i}(h_n t)$ for $h_i = 0$ and $h_n t > 0$ in Figs. 2(a) and 2(b) for $\Delta = 0$ and $\Delta = 0.1$ [45], respectively.

Equation (2) suggests that the onset of the the q.s. regime scales with h_n as $t_{qs} \propto h_n^{-1}$, hence the duration of the prethermal regime follows $\Delta t \equiv t_{qs} - t_{pt} \propto h_n^{-1}$. As the energy of the zero-momentum state in the integrable TFIC is $\epsilon_{k=0} = h_n$ [46], the prethermal duration $\Delta t \propto \epsilon_{k=0}^{-1}$ is inversely proportional to the single-particle energy gap. The prethermal regime lasts longer as we approach the QCP, motivating the name *critically prethermal regime* and justifying $\delta C_r(t, h_n)$ as the critical response.

In the following, we analytically derive $f_{\Delta,h_i}(h_n t)$ for the edge magnetization at $\Delta = 0$ and $h_i = 0$, and numerically demonstrate that it holds true for different probe sites r.

Prethermal regime in the integrable TFIC. The edge magnetization has an analytic series expression whose derivation

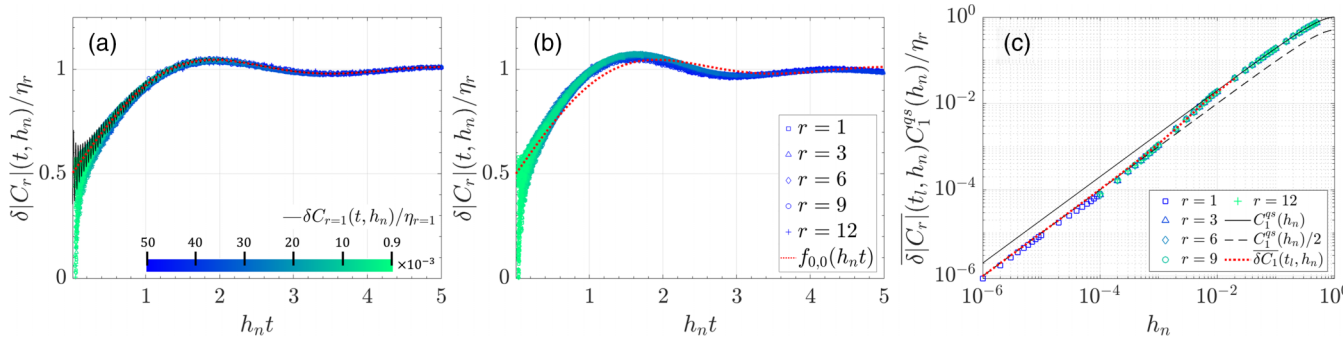

FIG. 2. Numerical rescaled critical response $\delta|C_r|(t,h_n)/\eta_r$ for (a) $\Delta=0$, the integrable TFIC and (b) $\Delta=0.1$, a near-integrable TFIC quenched from $h_i=0$ to $h_n\in[9\times10^{-4},0.05]$ (color bar). Here we plot data of 15 different h_n in (a) and 19 different h_n in (b) for each r. The system size is $N=1440$ and the numerical data are for probe sites $r=1,3,6,9,12$. The rescaling factor $\eta_r=C_1^{qs}(h_n)\delta|C_r|(t',h)/\delta|C_1|(t',h)$ is independent of the choice of t' and can be understood as the numerical evaluation of the q.s. value $C_r^{qs}(h_n)$. For the plots $t'=280$. As a comparison, the analytical value of $\delta C_1(t,h_n)/C_1^{qs}(h_n)$ (black-solid) is plotted in (a), and $f_{0,0}(h_n t)=f(h_n t)$ in Eq. (4b) (red-dotted) is plotted in both (a) and (b). (c) The dynamical order parameter for the integrable TFIC with cutoffs $t^*=20$ and $t_l=330$. The numerical data for different r collapse on top of $\overline{\delta C_1}(t_l,h_n)$, Eq. (6) (red-dotted). When t_l is in the decay ($t_l h_n\gg1$) or q.s. ($t_l h_n\ll1$) regimes, the data are described by $C_1^{qs}(h_n)/2$ (dashed-black line) and $C_1^{qs}(h_n)$ (solid-black line), respectively, both linear in h_n when $h_n\ll1$. When t_l is in the prethermal regime ($h_n t_l\sim1$), the data deviate from the linear functions in the two ends.

can be found in [40]

$$C_1(t,h)=1+\sum_{m=1}^{\infty}\frac{(-1)^m}{(2m)!}(2t)^{2m}N_m(h^2),$$

$$N_m(h^2)=\sum_{n=1}^{m}N_{mn}h^{2n},\quad N_{mn}=\frac{1}{m}\binom{m}{n-1}\binom{m}{n},\tag{3}$$

where $N_m(x)$ are the Narayana polynomials [47,48]. Equation (3) also describes the two-time edge correlators in the Kitaev chain at infinite temperature [30]. It has an analytical expression $C_1(t,h=1)=J_1(4t)/(2t)$ at the QCP [40] where $J_1(t)$ is the Bessel function of the first kind. Additionally, we note that Eq. (3) is a generating function of the Narayana polynomials and can be expressed in terms of the inverse Laplace transform of a closed form function [49]. This alternative expression is useful in probing the critically prethermal regime and deriving $f_{\Delta,h_i}(h_n t)$. The critical response in the vicinity of the QCP $h_n\to0$ follows [49]

$$\delta C_1(t,h_n)=C_1^{qs}(|h_n|)\left[-\frac{1}{2}J_0(4t)+f(h_n t)\right]+O\left(h_n^2\right),\tag{4a}$$

$$f(h_n t)\equiv\frac{1}{2}-\sum_{n=1}^{\infty}\frac{(-h_n t)^{2n-1}}{(2n)!}\chi_n,\tag{4b}$$

where $\chi_n\equiv(-1)^{1-n}(2n-2)!/(n-1)!^2$. $\delta C_1(t,h_n)/C_1^{qs}(h_n)$ for $h_n=0.005$ based on Eq. (4a) is plotted as a black-solid line in Fig. 2(a). Here the term $-\frac{1}{2}C_1^{qs}(|h_n|)J_0(4t)$, where $J_0(t)$ is the Bessel function of the first kind, introduces oscillations that become negligible when $t\gg1$. This term also originates from a high frequency expansion in the derivation [49], which is why it is only an early-time effect and hence nonuniversal. The function $f(h_n t)$ can be written in terms of a generalized Hypergeometric function $f(h_n t)=\frac{1}{2}+\frac{(h_n t)}{2}{}_1F_2[\{\frac{1}{2}\};\{\frac{3}{2},2\};-(h_n t)^2]$ [49] and it is plotted in Fig. 2(a) with a dotted-red line. In contrast to the nonuniversal term, $f(h_n t)$ originates from a low frequency —long-wavelength— expansion in the derivation, and hence providing extra evidence that the prethermal regime is critical. Let us note in passing that the rescaling of time with h_n that emerges from the microscopic calculation is consistent with the Ising universality class ($\nu=z=1$) [46].

Next we demonstrate Eq. (2) in the ordered phase using numerics for a finite-size system ($N=1440$). Because our numerics are based on the cluster theorem in the space-time limit [38], we obtain numerical values of $|C_r(t,h_n)|$, and hence use $\delta|C_r|(t,h_n)\equiv||C_r(t,h_n)|-|C_r(t,0)||$ to approximate $\delta C_r(t,h_n)$ [40,50]. Our numerical data show that, for $h_n\to0$, and $t\gg1$, $\delta C_r(t,h)$ for different choices of r are proportional to each other. Hence defining $\eta_r=C_1^{qs}(h_n)\delta|C_r|(t',h_n)/\delta|C_1|(t',h_n)$, we find numerically that η_r does not depend on t' as long as $t'\gg1$ [51]. For the edge spin, $\eta_1=C_1^{qs}(h_n)$ by definition. The authors of Refs. [43,52] showed that the q.s. values of the bulk spins have an exponentially decaying spatial profile in r, suggesting $\eta_r\approx C_1^{qs}(h_n)e^{-(r-1)/\xi(h_n)}$, where $\xi(h_n)$ is the correlation length [49]. Then the q.s. regime value at any r tends to zero linearly in h_n as $h_n\to0$.

Figure 2(a) plots $\delta|C_r|(t\geqslant50,h_n)/\eta_r$ for all $r=1,3,6,9,12$ quenched from an initial state $h_i=0$ to $h_n\in[9\times10^{-4},0.05]$. The colors, from dark blue to light cyan, correspond to decreasing h_n, respectively. The time axis is rescaled by the distance to the QCP, h_n. For Fig. 2(a), $t'=280$ is chosen in η_r. The data collapse on top of each other, and match well with the analytical function $f(h_n t)$ for $h_n t\gg0.1$. Therefore, we numerically demonstrate the validity of Eq. (2) for different probe sites $r>1$ in the ordered phase, and hence $f_{0,0}(h_n t)=f(h_n t)$.

Discussion for $\Delta, h_i\neq0$. In this section, we discuss Eq. (2) and $f_{\Delta,h_i}(h_n t)$ for general Δ and h_i. We present the case of $\Delta=0.1$ as an example of the near-integrable model which can be treated with quench mean-field theory (qMFT) [40,45]. In this case, the QCP is shifted to $h_c\approx1.165$ and numerical evidence shows that the location of the nonanalyticity observed in the dynamical order parameter is no longer equal to the QCP [40]. Hence in Ref. [40], some of us defined a dynamical critical point (DCP) based on the nonanalyticity following Ref. [27], and find it to be $h_{dc}=1.1437$. Since qMFT maps

the interacting problem back to a noninteracting problem, we also applied single-particle energy gap analysis in Ref. [40], and show that the gap for this noninteracting model indeed closes at $h_{dc} = 1.1437$. Therefore, it is natural to anticipate that a possible critically prethermal regime should emerge around h_{dc} for $\Delta \neq 0$, motivating a definition of the reduced control parameter as $h_n = (h_{dc} - h)/h_{dc}$.

Figure 2(b) verifies Eq. (2) for $\Delta = 0.1$ in the ordered phase using qMFT numerics for $r = 1, 3, 6, 9, 12$ quenched from an initial state $h_i = 0$ to $h_n \in [8.74 \times 10^{-4}, 0.0557]$. Our joint work [40] showed that for small Δ, $C_1^{qs}(h) = \alpha(h_{dc}^{\nu} - h^{\nu})$ where α and ν were numerically extracted as $\alpha = 0.81$ and $\nu = 1.81$ for $\Delta = 0.1$. Note that for $\alpha = 1, \nu = 2$, and $h_{dc} = h_c = 1$, we recover the q.s. value of the edge spin in the integrable TFIC $C_1^{qs}(h) = 1 - h^2$. Hence, $C_1^{qs}(h_n) = \alpha h_{dc}^{\nu}[1 - (1 - h_n)^{\nu}]$ and we use this expression to define η_1. η_r for $r \neq 1$ are defined similarly as in the integrable case. Importantly, we find that all data for $\delta|C_r|(t \geqslant 50, h_n)/\eta_r$ collapse on top of each other, which confirms the validity of Eq. (2) for small $\Delta \neq 0$. However, the data does not match with the function $f_{0,0}(h_n t)$ [red-dotted line in Fig. 2(b)], suggesting that $f_{\Delta,h_i}(h_n t)$ depends on Δ. In the Supplemental Material (SM), we verify Eq. (2) numerically for $h_i \neq 0$ and show that $f_{\Delta,h_i}(h_n t)$ also depends on h_i [49].

For all Δ, h_i, and r considered, $C_r^{qs}(|h_n|) \sim |h_n|$ as $h_n \to 0$. Specifically, when $\Delta = 0$, $C_r^{qs}(|h_n|) = 2^{2-r}|h_n| + O(|h_n^{3/2}|)$ for $\Delta = 0$, and $C_1^{qs}(h_n) \approx \alpha\nu h_{dc}^{\nu} h_n$ for $\Delta = 0.1$. The case of $h_i \neq 0$ was discussed in Ref. [40]. The linear scaling of $C_r^{qs}(|h_n|)$ in h_n results in the self-similarity of the critical response: When $h_n \to 0$, $t \gg 1$ and $\kappa t \gg 1$, $\delta C_r(t, h_n) = \kappa \delta C_r(\kappa^{-1} t, \kappa h_n)$ where κ is a rescaling factor.

Scaling of dynamical order parameter near QCP. Finally, we probe the critically slowed down prethermal regime in the ordered phase ($h_n > 0$) by studying the scaling of a dynamical order parameter defined with a finite long-time cutoff t_l:

$$\overline{\delta C_r}(t_l, h_n) \equiv \frac{1}{t_l - t^*} \int_{t^*}^{t_l} dt\ \delta C_r(t, h_n), \tag{5}$$

where t^* is a short-time cutoff with negligible influence on the value of $\overline{\delta C_r}(t_l, h_n)$ [49]. This newly introduced dynamical order parameter extends beyond the current paradigm of probing the dynamical scaling near a QCP at infinite time and enables the discussion of experiments often limited by finite coherence times. Here we can imagine t_l as the experimentally (or computationally) longest time accessible. The temporal cutoff can be extended to $t_l \to \infty$ if desired.

When $t^* = 0$, Eq. (4b) together with Eq. (2) suggest that the dynamical order parameter for $\Delta = 0$ and $h_i = 0$ is given by [53]

$$\overline{\delta C_r}(t_l, h_n) = C_r^{qs}(|h_n|)\left[\frac{1}{2} - \sum_{n=1}^{\infty} \frac{(-h_n t_l)^{2n-1}}{2n \times (2n)!}\chi_n\right] + O\big(h_n t_l^{-1}\big) + O\big(h_n^2\big). \tag{6}$$

$\overline{\delta C_r}(t_l, h_n)$ for $r = 1$ is plotted in Fig. 2(c) as the red-dotted line for $t_l = 330$. When $t_l \gg 1$ and $h_n \to 0$, the first line of Eq. (6) gives a good approximation of $\overline{\delta C_r}(t_l, h_n)$. For $h_n t_l \ll 1$ and $h_n t_l \gg 1$, t_l probes the beginning of the prethermal ramp and the q.s. regime, respectively. In these regimes, we observe $\overline{\delta C_1}(t_l, h_n) \approx \frac{1}{2} C_1^{qs}(h_n)$ (dashed-black) and $\overline{\delta C_1}(t_l, h_n) \approx C_1^{qs}(h_n) = 1 - (1 - h_n)^2$ (solid-black), respectively. Both are linear in h_n for $h_n \ll 1$ and connected through a nonlinear crossover when $h_n t_l \sim 1$ holds and hence when t_l probes the prethermal ramp.

Similar to the previous discussion, we numerically define $\overline{\delta|C_r|}(t_l, h_n)$ as the time average of $\delta|C_r|(t, h_n)$ between t^* and t_l. To demonstrate that the dynamical order parameter has a similar scaling behavior for different r, we rescale the data using η_r and plot $\overline{\delta|C_r|}(t_l, h_n) C_1^{qs}(h_n)/\eta_r$ in Fig. 2(c). Note that $\overline{\delta|C_r|}(t_l, h_n) C_1^{qs}(h_n)/\eta_r = \overline{\delta|C_r|}(t_l, h_n)$ for $r = 1$ by definition. The linear-to-linear crossover in $\overline{\delta C_r}(t_l, h_n)$ for small $h_n > 0$, demonstrated in Fig. 2(c), is universal for any Δ and h_i, and robust against changing t_l [49], while the shape of the nonlinear crossover depends on $f_{\Delta,h_i}(h_n t)$. This is suggested by Eq. (2), where $f_{\Delta,h_i}(h_n t)$ has universal limiting properties and $C_r^{qs}(h_n)$ always has linear scaling in h_n. To demonstrate the universality, we plot the numerical data of $\overline{\delta|C_r|}(t_l, h_n) C_1^{qs}(h_n)/\eta_r$ for $\Delta = 0.1, h_i = 0$, and $\Delta = 0, h_i = 0.1$ in the SM [49].

Conclusion and outlook. We discover critical slowing down in the open-boundary TFIC upon suddenly quenching to the vicinity of the QCP. This critical slowing down is expressed in Eq. (2) universally for any probe site, weak interactions, or the initial state, and rigorously proven for a special case. Analytical analysis leads us to reveal self-similarity in the dynamics and find that the duration of the prethermal regime diverges as one approaches the QCP because of the gap closing. The critically prethermal regime in the near-integrable TFIC is also evident in time-dependent density-matrix renormalization group calculations [54]. Therefore our conclusions for weakly interacting TFIC seem to be valid beyond the qMFT method. An interesting question to answer in the future is whether Eq. (2) is applicable in strongly interacting TFIC.

Emerging dynamical universality in suddenly quenched TFIC suggests the presence of critical slowing down in other open-boundary short-range spin chains, e.g., the XXZ chain [36]. Critical slowing down should also be manifested in other system observables that host a late-time nonanalyticity in their sudden quench dynamics [27]. Whether the critical slowing down in sudden quench dynamics holds generically beyond the Ising universality class, poses an exciting prospect for future studies.

Acknowledgments. We thank Susanne Yelin for helpful discussion. C.B.D. acknowledges support from the NSF through a grant for ITAMP at Harvard University. Y.W. is supported by AFOSR and NSF. J.C.H. and P.U. acknowledge funding from the European Research Council (ERC) under the European Union's Horizon 2020 research and innovation programme (Grant Agreement No. 804305), the Provincia Autonoma di Trento, support from Q@TN, the joint lab between University of Trento, FBK–Fondazione Bruno Kessler, INFN–National Institute for Nuclear Physics and CNR–National Research Council, as well as the Collaborative Research Centre ISOQUANT (Project No. 273811115).

[1] J. Eisert, M. Friesdorf, and C. Gogolin, Nat. Phys. **11**, 124 (2015).

[2] M. Greiner, O. Mandel, T. Esslinger, T. W. Hänsch, and I. Bloch, Nature (London) **415**, 39 (2002).

[3] W. S. Bakr, J. I. Gillen, A. Peng, S. Fölling, and M. Greiner, Nature (London) **462**, 74 (2009).

[4] M. Cheneau, P. Barmettler, D. Poletti, M. Endres, P. Schauß, T. Fukuhara, C. Gross, I. Bloch, C. Kollath, and S. Kuhr, Nature (London) **481**, 484 (2012).

[5] R. Islam, R. Ma, P. M. Preiss, M. E. Tai, A. Lukin, M. Rispoli, and M. Greiner, Nature (London) **528**, 77 (2015).

[6] A. M. Kaufman, M. E. Tai, A. Lukin, M. Rispoli, R. Schittko, P. M. Preiss, and M. Greiner, Science **353**, 794 (2016).

[7] J. Zhang, G. Pagano, P. W. Hess, A. Kyprianidis, P. Becker, H. Kaplan, A. V. Gorshkov, Z.-X. Gong, and C. Monroe, Nature (London) **551**, 601 (2017).

[8] M. Gärttner, J. G. Bohnet, A. Safavi-Naini, M. L. Wall, J. J. Bollinger, and A. M. Rey, Nat. Phys. **13**, 781 (2017).

[9] A. Keesling, A. Omran, H. Levine, H. Bernien, H. Pichler, S. Choi, R. Samajdar, S. Schwartz, P. Silvi, S. Sachdev *et al.*, Nature (London) **568**, 207 (2019).

[10] P. Scholl, M. Schuler, H. J. Williams, A. A. Eberharter, D. Barredo, K.-N. Schymik, V. Lienhard, L.-P. Henry, T. C. Lang, T. Lahaye *et al.*, Nature (London) **595**, 233 (2021).

[11] S. Ebadi, T. T. Wang, H. Levine, A. Keesling, G. Semeghini, A. Omran, D. Bluvstein, R. Samajdar, H. Pichler, W. W. Ho *et al.*, Nature (London) **595**, 227 (2021).

[12] T. Mori, T. N. Ikeda, E. Kaminishi, and M. Ueda, J. Phys. B: At., Mol. Opt. Phys. **51**, 112001 (2018).

[13] M. Heyl, A. Polkovnikov, and S. Kehrein, Phys. Rev. Lett. **110**, 135704 (2013).

[14] N. Tsuji, M. Eckstein, and P. Werner, Phys. Rev. Lett. **110**, 136404 (2013).

[15] P. Jurcevic, H. Shen, P. Hauke, C. Maier, T. Brydges, C. Hempel, B. P. Lanyon, M. Heyl, R. Blatt, and C. F. Roos, Phys. Rev. Lett. **119**, 080501 (2017).

[16] N. Fläschner, D. Vogel, M. Tarnowski, B. S. Rem, D.-S. Lühmann, M. Heyl, J. C. Budich, L. Mathey, K. Sengstock, and C. Weitenberg, Nat. Phys. **14**, 265 (2018).

[17] B. Sciolla and G. Biroli, Phys. Rev. B **88**, 201110(R) (2013).

[18] E. Nicklas, M. Karl, M. Höfer, A. Johnson, W. Muessel, H. Strobel, J. Tomkovič, T. Gasenzer, and M. K. Oberthaler, Phys. Rev. Lett. **115**, 245301 (2015).

[19] A. Chiocchetta, M. Tavora, A. Gambassi, and A. Mitra, Phys. Rev. B **91**, 220302(R) (2015).

[20] V. Gurarie, Phys. Rev. A **100**, 031601(R) (2019).

[21] C. B. Dağ and K. Sun, Phys. Rev. B **103**, 214402 (2021).

[22] D. Trapin, J. C. Halimeh, and M. Heyl, Phys. Rev. B **104**, 115159 (2021).

[23] C. Kollath, A. M. Läuchli, and E. Altman, Phys. Rev. Lett. **98**, 180601 (2007).

[24] M. Karl, H. Cakir, J. C. Halimeh, M. K. Oberthaler, M. Kastner, and T. Gasenzer, Phys. Rev. E **96**, 022110 (2017).

[25] M. Heyl, F. Pollmann, and B. Dóra, Phys. Rev. Lett. **121**, 016801 (2018).

[26] H.-X. Yang, T. Tian, Y.-B. Yang, L.-Y. Qiu, H.-Y. Liang, A.-J. Chu, C. B. Dağ, Y. Xu, Y. Liu, and L.-M. Duan, Phys. Rev. A **100**, 013622 (2019).

[27] P. Titum, J. T. Iosue, J. R. Garrison, A. V. Gorshkov, and Z.-X. Gong, Phys. Rev. Lett. **123**, 115701 (2019).

[28] P. Uhrich, N. Defenu, R. Jafari, and J. C. Halimeh, Phys. Rev. B **101**, 245148 (2020).

[29] A. Haldar, K. Mallayya, M. Heyl, F. Pollmann, M. Rigol, and A. Das, Phys. Rev. X **11**, 031062 (2021).

[30] F. J. Gómez-Ruiz, J. J. Mendoza-Arenas, F. J. Rodríguez, C. Tejedor, and L. Quiroga, Phys. Rev. B **97**, 235134 (2018).

[31] C. B. Dağ, L.-M. Duan, and K. Sun, Phys. Rev. B **101**, 104415 (2020).

[32] Z.-H. Sun, J.-Q. Cai, Q.-C. Tang, Y. Hu, and H. Fan, Ann. Phys. (Leipzig) **532**, 1900270 (2020).

[33] J. Dziarmaga, Adv. Phys. **59**, 1063 (2010).

[34] A. Polkovnikov, K. Sengupta, A. Silva, and M. Vengalattore, Rev. Mod. Phys. **83**, 863 (2011).

[35] M. Eckstein, M. Kollar, and P. Werner, Phys. Rev. Lett. **103**, 056403 (2009).

[36] P. Barmettler, M. Punk, V. Gritsev, E. Demler, and E. Altman, Phys. Rev. Lett. **102**, 130603 (2009).

[37] M. Eckstein, M. Kollar, and P. Werner, Phys. Rev. B **81**, 115131 (2010).

[38] P. Calabrese, F. H. L. Essler, and M. Fagotti, J. Stat. Mech.: Theory Exp. (2012) P07016.

[39] $C_1(t)$ in Fig. 1 can be plotted using either an alternative expression for Eq. (3) or the inverse Laplace transform expression detailed in [49], as evaluating the series summation in Eq. (3) for long times becomes virtually impossible.

[40] C. B. Dağ, P. Uhrich, Y. Wang, I. P. McCulloch, and J. C. Halimeh, Phys. Rev. B **107**, 094432 (2023).

[41] P. Calabrese and J. Cardy, Phys. Rev. Lett. **96**, 136801 (2006).

[42] P. Calabrese, F. H. L. Essler, and M. Fagotti, Phys. Rev. Lett. **106**, 227203 (2011).

[43] F. Iglói and H. Rieger, Phys. Rev. Lett. **106**, 035701 (2011).

[44] F. Iglói, G. Roósz, and Y.-C. Lin, New J. Phys. **15**, 023036 (2013).

[45] The near-integrable model is mapped to the single-particle picture and the dynamics are calculated via quench mean-field theory (qMFT). qMFT introduces next n.n. coupling and pairing to the usual Kitaev chain and simply renormalizes the n.n. coupling and pairing strengths J as well as the chemical potential h. Hence, the QCP shifts favoring order. For details of this method and the results, see [40].

[46] S. Sachdev, *Quantum Phase Transitions* (Cambridge University Press, Cambridge, England, 2001).

[47] V. P. Kostov, A. Martinez-Finkelshtein, and B. Z. Shapiro, J. Approx. Theory **161**, 464 (2009).

[48] T. Mansour and Y. Sun, Discrete Math. **309**, 4079 (2009).

[49] See Supplemental Material at http://link.aps.org/supplemental/10.1103/PhysRevB.107.L121113 for analytical derivation of Eqs. 4(a) and 4(b), numerical verification of Eq. (2) and more numerical results on the critical response and dynamical order parameter, which also include Refs. [55,56].

[50] This is a good approximation when $C_r(t, h_n)$ and $C_r(t, 0)$ are both positive, hence it is expected to work well only in the ordered phase. This approximation is also the reason why we observe a mismatch between numerics and analytics in Fig. 2(a) for the values $h_n t \ll 1$.

[51] This indicates that when $t' \geqslant t_{qs}$, $\eta_r = \delta C_r(t = \infty, h_n) = C_r^{qs}(h_n)$ can be used to numerically extract the q.s. value

of spin r from finite-time data [using the fact that $C_r(t = \infty, h = 1) = 0$].
[52] K. Sengupta, S. Powell, and S. Sachdev, Phys. Rev. A **69**, 053616 (2004).
[53] Equation (6) can also be expressed as a hypergeometric function [49].
[54] See Figs. 22(b) and 23(b) in our joint paper [40].
[55] T. Petersen, *Eulerian Numbers*, Birkhäuser Advanced Texts Basler Lehrbücher (Springer, New York, 2015).
[56] R. Graham, D. Knuth, and O. Patashnik, *Concrete Mathematics: A Foundation for Computer Science* (Addison-Wesley, New York, 1994).